Okamoto, Y., & Yount, R. G. (1985b) 11th Yamada Conference on Energy Transduction in ATPases, May 27–31, Kobe, Japan.
Pemrick, S., & Weber, A. (1976) *Biochemistry 15*, 5193–5198.
Prince, H. P., Trayer, H. R., Henry, G., Trayer, I. P., Dalgarno, D. C., Levine, B. A., Cary, P. D., & Turner, C. (1981) *Eur. J. Biochem. 121*, 213–216.
Sivaranakrishnan, M., & Burke, M. (1982) *J. Biol. Chem. 257*, 1102–1105.
Sutoh, K. (1982) *Biochemistry 21*, 3654–3661.
Sutoh, K. (1983) *Biochemistry 22*, 1579–1585.
Szilagyi, L., Balint, M., Streter, F. A., & Gergely, J. (1979) *Biochem. Biophys. Res. Commun. 87*, 936–945.
Taylor, E. W. (1979) *CRC Crit. Rev. Biochem. 6*, 102–164.
Wagner, P. D., & Weed, A. G. (1979) *Biochemistry 18*, 2260–2266.
Wagner, P. D., & Giniger, E. (1981) *Nature (London) 292*, 560–561.
Walker, J. E., Saraste, M., Runswick, M. J., & Gray, N. J. (1982) *EMBO J. 1*, 945–951.
Webb, M. R., Ash, D. E., Leyh, T. S., Trentham, D. R., & Reed, G. M. (1982) *J. Biol. Chem. 257*, 3068–3072.
Weeds, A. G., & Taylor, R. S. (1975) *Nature (London) 257*, 54–56.
Winstanley, M. A., Small, D. A., & Trayer, I. P. (1979) *Eur. J. Biochem. 98*, 441–446.

# Effect of Temperature on the Mechanism of Actin Polymerization†

Chris T. Zimmerle and Carl Frieden*
*Department of Biological Chemistry, Washington University School of Medicine, St. Louis, Missouri 63110*
*Received May 7, 1986; Revised Manuscript Received July 2, 1986*

ABSTRACT: The rate of the $Mg^{2+}$-induced polymerization of rabbit skeletal muscle G-actin has been measured as as function of temperature at pH 8 by using various concentrations of $Mg^{2+}$, $Ca^{2+}$, and G-actin. A polymerization mechanism similar to that proposed at this pH [Frieden, C. (1983) *Proc. Natl. Acad. Sci. U.S.A. 80*, 6513–6517] was found to fit the data from 10 to 35 °C. From the kinetic data, no evidence for actin filament fragmentation was found at any temperature. Dimer formation is the most temperature-sensitive step, with the ratio of forward and reverse rate constants changing 4 orders of magnitude from 10 to 35 °C. Over this temperature change, all other ratios of forward and reverse rate constants change 7-fold or less, and the critical concentration remains nearly constant. The reversible $Mg^{2+}$-induced isomerization of G-actin monomer occurs to a greater extent with increasing temperature, measured either by using *N*-(iodoacetyl)-*N'*-(5-sulfo-1-naphthyl)ethylenediamine-labeled actin or by simulation of the full-time course of the polymerization reaction. This is partially due to $Mg^{2+}$ binding becoming tighter, and $Ca^{2+}$ binding becoming weaker, with increasing temperature. Elongation rates from the filament-pointed end, determined by using actin nucleated by plasma gelsolin, show a temperature dependence slightly larger than that expected for a diffusion-limited reaction.

Actin can undergo transformation from a monomeric form (G-actin) to a long helical polymer (F-actin)[1] by a polymerization process classically described as a nucleation–elongation reaction (Oosawa & Kasai, 1962). This polymerization process in vitro is strongly influenced by environmental variables such as pH, temperature, and ionic strength (Kasai et al., 1962; Kasai, 1969), and actin assembly or disassembly in vivo is probably influenced by similar factors as well as by actin binding proteins. Thus, detailed knowledge of the role such environmental factors play may be important for understanding the regulation and modulation of in vivo actin polymerization.

The temperature-dependent studies of actin polymerization to date have involved measuring the changes in either critical concentration ($C_c$), viscosity, or polymerization half-time (Swezey & Somero, 1982; Grazi & Trombetta, 1985; Kasai et al., 1962). Viscosity measurements, however, result in artificial filament fragmentation due to shear stresses, thereby increasing the filament number and polymerization rate. The polymerization half-time appears to be an inadequate reflection of the overall polymerization mechanism (Frieden & Goddette, 1983), while critical concentration measurements may depend upon conditions used and do not necessarily reflect only the monomer–filament equilibrium (Frieden, 1983, 1985). Thus, none of these methods has reliably characterized the full polymerization time course nor given any clues as to the mechanism.

In recent years, the use of fluorescently labeled actins has been found to yield a more sensitive and accurate measurement of actin polymerization and/or conformation [a review of these probes is given in Tait & Frieden (1983)]. Changes in the fluorescence of AEDANS-labeled actin have previously been shown to be related to a $Mg^{2+}$-induced isomerization of G-actin

† This work was supported in part by Grant AM 13332 from the National Institutes of Health.
* Address correspondence to this author.

[1] Abbreviations: Ca–G-actin, monomeric actin with bound $Ca^{2+}$; Mg–G-actin, monomeric actin with bound $Mg^{2+}$; F-actin, polymerized filamentous actin; AEDANS-labeled actin, actin labeled with *N*-(iodoacetyl)-*N'*-(5-sulfo-1-naphthyl)ethylenediamine; pyrene-labeled actin, actin labeled with *N*-(1-pyrenyl)iodoacetamide; Tris, tris(hydroxymethyl)aminomethane.

0006-2960/86/0425-6432$01.50/0 

(Frieden et al., 1980). This proposed $Mg^{2+}$-induced conformational change has been supported by both immunological methods (Roustan et al., 1985) and proton NMR spectroscopy (Barden & Remedios, 1985). Further, the incorporation of G-actin monomer into F-actin results in a large fluorescence enhancement of pyrene-labeled actin which is directly related to actin polymerization (Tellam & Frieden, 1983; Cooper et al., 1983; Frieden, 1983; Kouyama & Mihashi, 1980).

Complete polymerization mechanisms proposed to date have generally involved a monomeric activation step, followed by nucleation and elongation, and finally possible filament fragmentation (Frieden, 1983; Pantaloni et al., 1985; Wegner & Savko, 1982; Cooper et al., 1983). The basis for these steps follows that of previous work on actin nucleation (Oosawa & Kasai, 1962; Wegner & Engel, 1975) and elongation (Pollard & Mooseker, 1981; Bonder et al., 1983).

In this paper, we examine the temperature dependence of actin polymerization. The data appear to follow the polymerization scheme described previously by Frieden (1983). In this mechanism, $Mg^{2+}$ and $Ca^{2+}$ compete for an identical high-affinity binding site on the actin molecule, with $Mg^{2+}$ addition inducing an actin monomer conformational change necessary for the $Mg^{2+}$-dependent polymerization. This is followed by binding of $Mg^{2+}$ to a second low-affinity site on the actin molecule. This form of $Mg^{2+}$–actin then associates to form oligomers which serve as nuclei from which subsequent rapid elongation can occur. We have obtained rate constants which describe this polymerization process and have examined how these rate constants change with temperature. These rate constants were obtained by using pyrene-labeled actin for the transformation of G-actin to F-actin and AEDANS-labeled actin for monitoring the $Mg^{2+}$-induced conformational change.

## Materials and Methods

*Protein Purification and Modification.* Rabbit muscle G-actin was purified by the method of Spudich and Watt (1971), modified as described previously (Frieden et al., 1980). Plasma gelsolin (brevin) was prepared from rabbit plasma, purchased from Pel-Freeze, according to the method of Harris and Weeds, modified as described by Doi and Frieden (1984).

Pyrene-labeled actin was prepared by a modification (Tellam & Frieden, 1982) of the method of Kouyama and Mihashi (1980). AEDANS-labeled actin was labeled by a procedure similar to that of Tawada et al. (1978) modified slightly (Frieden et al., 1980). The molar ratio of dye/actin for either fluorescently labeled actin was between 0.8 and 0.95. Both fluorophores are known to covalently modify cysteine-374 (Kouyama & Mihashi, 1980). If the actin was not immediately used, 2 mg/mL sucrose was added per milligram of actin; the solution was lyophilized and stored at −20 °C. To prepare Ca–G-actin, lyophilized powders were dissolved and dialyzed for at least 15 h against G buffer (2 mM Tris-HCl, pH 8, 200 $\mu$M $Ca^{2+}$, 200 $\mu$M ATP, and 1.5 mM $NaN_3$), adjusted to correct for temperature-induced pH changes. Mg–G-actin was prepared by further dialysis of G-actin against Tris buffer containing 200 $\mu$M ATP, 50 $\mu$M $Mg^{2+}$, and 1.5 mM $NaN_3$. Protein concentrations were determined spectrophotometrically by using $A_{1mg/mL} = 0.63$ at 290 nm (Houk & Ue, 1974) or by the method of Bradford (1976) using G-actin as a standard. Prior to use, all actin solutions were centrifuged for 100000$g$ for 1 h or at 180000$g$ for 30 min.

*Polymerization Studies.* Actin polymerization was monitored by using trace amounts of pyrene-labeled (<1%) actin as described elsewhere (Tellam & Frieden, 1982), while the $Mg^{2+}$-induced conformational change was followed by using AEDANS-labeled actin as described previously (Frieden et al., 1980). For polymerization reactions using Mg–G-actin, 250 $\mu$M $Mg^{2+}$ was added 5 min before the initialization of polymerization. This prior incubation with a low level of $Mg^{2+}$ ensured most actin is in the conformer represented by A′Mg in Scheme I but fails to induce any polymerization as detected by the absence of any fluorescence enhancement of the pyrene-labeled actin during the incubation time. Thus, polymerization of Mg–G-actin does not involve steps 1 and 2 of Scheme I. For experiments measuring filament elongation, 15 $\mu$M actin was incubated 5 min with 0.3 or 0.15 $\mu$M plasma gelsolin, 250 $\mu$M $Mg^{2+}$, and 50 $\mu$M $Ca^{2+}$ and then polymerized by the addition of 10 mM $Mg^{2+}$. The amount of $Ca^{2+}$ added is necessary for plasma gelsolin activity (Harris & Weeds, 1983). All the polymerization reactions at a given experimental condition were repeated on different days to ensure time courses obtained were reproducible.

*Fluorescence Experiments.* Static fluorescence studies were performed on a Spex spectrofluorometer in the E/R mode. This mode corrects for any signal fluctuations as a result of changes in the excitation light intensity. For experiments utilizing AEDANS-labeled actin, excitation and emission wavelengths of 340 and 460 nm, respectively, were used. For experiments utilizing pyrene-labeled actin, excitation and emission wavelengths of 365 and 386 nm were used. Stopped-flow fluorescence measurements of AEDANS-labeled actin were obtained by using a Durrum stopped-flow apparatus in the fluorescence mode with an excitation wavelength of 340 nm. A Corning 0-52 filter placed before the photomultiplier tube adsorbed all scattered incident light while fully transmitting fluorescent light at wavelengths greater than 400 nm. Data from both stopped-flow and static fluorescence studies were collected continuously and stored in digital mode for later recall.

*Data Analysis.* The mechanism used to fit the polymerization time courses at all temperatures was one used previously to fit actin polymerization at pH 8 and 20 °C (Frieden, 1983) and is described in Scheme I. In Scheme I, monomeric G-actin is represented by A, G-actin containing bound $Ca^{2+}$ by ACa, G-actin containing one bound $Mg^{2+}$ by AMg, and actin monomer which has undergone the Mg-induced conformational change by A′Mg. $K_{Mg•}$ describes the initial binding to the first $Mg^{2+}$ site, $K_{Mg1}$ describes the overall binding ($K_{Mg•}k_{-1}/k_{+1}$) of $Mg^{2+}$ to this site, and $K_{Mg2}$ describes $Mg^{2+}$ binding to the second binding site. The rate constants $k_{+e}$ and $k_{-e}$ in Scheme I describe the overall elongation and disassembly rates, respectively, of the F-actin filament.

Scheme I

$$A + Ca \underset{}{\overset{K_{Ca}}{\rightleftharpoons}} ACa \quad (1)$$

$$A + Mg \overset{K_{Mg•}}{\rightleftharpoons} AMg \underset{k_{-1}}{\overset{k_{+1}}{\rightleftharpoons}} A'Mg \quad (2)$$

$$A'Mg + Mg \overset{K_{Mg2}}{\rightleftharpoons} A'(Mg)_2 \quad (3)$$

$$2A'(Mg)_2 \underset{k_{-2}}{\overset{k_{+2}}{\rightleftharpoons}} \{A'(Mg)_2\}_2 \quad (4)$$

$$A'(Mg)_2 + \{A'(Mg)_2\}_2 \underset{k_{-3}}{\overset{k_{+3}}{\rightleftharpoons}} \{A'(Mg)_2\}_3 \quad (5)$$

$$A'(Mg)_2 + \{A'(Mg)_2\}_3 \underset{k_{-4}}{\overset{k_{+4}}{\rightleftharpoons}} \{A'(Mg)_2\}_4 \quad (6)$$

$$\vdots$$

$$A'(Mg)_2 + \{A'(Mg)_2\}_n \underset{k_{-e}}{\overset{k_{+e}}{\rightleftharpoons}} \{A'(Mg)_2\}_n \quad (7)$$

Kinetic parameters for the $Mg^{2+}$-induced conformational change were determined as follows: The $Mg^{2+}$-induced

Table I: Kinetic Parameters for the $Mg^{2+}$-Induced Conformational Change in G-Actin as a Function of Temperature[a]

| temp (°C) | $K_{Ca}$ ($\mu$M) | $K_{Mg^*}$[b] ($\mu$M) | $k_{+1}$ ($\mu M^{-1}$ $s^{-1}$) | $k_{-1}$ ($s^{-1}$) | $K_{Mg1}$[c] ($\mu$M) |
|---|---|---|---|---|---|
| 10 | 6 ± 2 | 1360 ± 520 | 0.15 ± 0.01 | 0.019 ± 0.003 | 171 |
| 20 | 10 ± 4 | 1100 ± 450 | 0.15 ± 0.02 | 0.011 ± 0.002 | 83 |
| 30 | 35 ± 9 | 880 ± 170 | 0.12 ± 0.01 | 0.006 ± 0.002 | 45 |

[a] Values reported were determined from stopped-flow experiments using AEDANS-labeled actin and analyzed as described under Materials and Methods. [b] Refers to the initial binding of $Mg^{2+}$, before the isomerization. [c] $K_{Mg1}$ refers to the apparent dissociation constant for the high-affinity $Mg^{2+}$ binding site of G-actin. This is equal to $(k_{-1}/k_{+1})K_{Mg^*}$.

time-dependent fluorescence enhancement of AEDANS-labeled actin (step 2 of Scheme I) was fit to a first-order rate equation. The first-order rate constants obtained ($k_{obsd}$) by this analysis were then used in fitting the equation:

$$k_{obsd} = k_{-1} + k_{+1}/\{1 + (K_{Mg^*}/[Mg^{2+}])(1 + [Ca^{2+}]/K_{Ca})\} \quad (1)$$

which has previously been used to obtain the rate and binding constants for the $Mg^{2+}$-induced conformational change (Frieden, 1982). Best fits of the data to each of these equations were determined by nonlinear regression programs written in the SAS (statistical analysis system) command language.

Computer simulations, utilizing Scheme I as the mechanism for actin polymerization, were performed by the program KINSIM on a Digital Electronics Corp. MicroVAX II. KINSIM allows simulation of kinetic mechanisms by numerical integration (Barshop et al., 1983). Simulations of actin polymerization in G buffer were made by assuming all actin initially in the G-actin monomeric form, as represented by ACa in Scheme I. Free $Ca^{2+}$ concentrations were assumed equal to the total $CaCl_2$ concentration present minus the actin concentration. Free $Mg^{2+}$ concentrations were assumed equal to the total $MgCl_2$ concentration present minus the ATP concentration. Although parameter values obtained are not the result of least-squares analysis, extensive manipulation of rate constants ensured the final simulations were unique fits to the real data. Generally less than a 10% change in any given parameter results in a noticeable degradation in fit between the observed and predicted time courses.

## Results

*Temperature Dependence of the $Mg^{2+}$-Induced Conformational Change.* The first approach toward analysis of the temperature dependence of actin polymerization involved analysis of the $Mg^{2+}$-induced conformational change, represented by steps 1 and 2 of Scheme I. As previously described (Frieden et al., 1980), addition of $Mg^{2+}$ to G-actin labeled with 1,5-AEDANS results in a first-order time-dependent fluorescence enhancement interpreted as the result of $Mg^{2+}$-dependent isomerization of actin (step 2 of Scheme I). The rate and dissociation constants derived from stopped-flow data of the fluorescence enhancement induced by the addition of varying concentrations of $Mg^{2+}$ (0.3–19.8 mM) to AEDANS-labeled G-actin at four different $Ca^{2+}$ concentrations (8, 10, 34, and 200 $\mu$M) at 10, 20, and 30 °C are shown in Table I. The values reported in Table I were obtained by fitting of the stopped-flow data to eq 1 as described under Materials and Methods. The same value for $k_{-1}$ was found by the addition of excess $Ca^{2+}$ (10 mM) to G-actin incubated with 200 $\mu$M ATP and 100 $\mu$M $Mg^{2+}$.

Static fluorescence studies of AEDANS-labeled actin indicated the base-line fluorescence before, as well as after, excess $Mg^{2+}$ addition decreased with temperature. This is expected for most fluorescence probes. However, fluorescence values before and after $Mg^{2+}$ addition decreased at different extents, such that a greater fluorescence enhancement is observed at higher temperature with $Mg^{2+}$ binding. The observed fluorescence enhancement at 30 °C induced by $Mg^{2+}$ addition increases by 1.2-fold over the observed enhancement at 10 °C and suggests a shift toward the formation of A'Mg.

*Temperature Dependence of Filament Elongation from the Pointed End.* Elongation from the filament-pointed end was investigated by using plasma gelsolin (brevin), a protein which caps the barbed end of actin filaments (Harris & Schwartz, 1983). This protein forms a complex with G-actin which serves as a nucleus for subsequent elongation from only the pointed end of the actin filament (Doi & Frieden, 1984).

Plasma gelsolin to actin ratios used were at or above the ratio which results in actin filament concentrations equivalent to the plasma gelsolin concentrations (Doi & Frieden, 1984). This allows the total filament concentration to be known, which is necessary for the calculation of the apparent elongation rate for the pointed or slow-growing end of the actin filament. A high $Mg^{2+}$ concentration (10 mM) was used to polymerize actin in these experiments to reduce the $Mg^{2+}$ dependence on the apparent elongation rate (Doi & Frieden, 1984). The apparent elongation rates found under the experimental conditions described, calculated as described by Doi and Frieden (1984), were 0.11, 0.29, and 0.65 $\mu mol^{-1}$ $s^{-1}$ at 10, 20, and 30 °C, respectively.

*Temperature Dependence of $Mg^{2+}$-Induced Polymerization.* To check and confirm the results found by using AEDANS-labeled actin, as well as to determine the rate constants for steps 3 through 7 of Scheme I, actin polymerization was monitored by using a trace amount of pyrene-labeled actin as described elsewhere (Tellam & Frieden, 1982). Actin polymerization as a function of free $Mg^{2+}$, Ca–G-actin, and Mg–G-actin concentrations was carried out between 10 and 35 °C. Rate constants and binding parameters determined by using AEDANS-labeled actin for the $Mg^{2+}$-induced isomerization of G-actin (Table I) were found to be adequate to achieve good fits between predicted (by Scheme I) and observed full polymerization time courses (Table II).

As shown in Figure 1, increasing temperature greatly increases the rate of polymerization while decreasing the amount

Table II: Kinetic Parameters for the $Mg^{2+}$-Induced Polymerization of Actin as a Function of Temperature[a]

| temp (°C) | $K_{Ca}$ ($\mu$M) | $K_{Mg^*}$ ($\mu$M) | $k_1$ ($\mu M^{-1}$ $s^{-1}$) | $k_{-1}$ ($s^{-1}$) | $K_{Mg2}$ ($\mu$M) | $k_{-2}$ ($\mu$M) | $k_{+3}$ ($\mu$M) | $k_{+e}$ ($\mu$M) |
|---|---|---|---|---|---|---|---|---|
| 10 | 6 | 1400 | 0.15 | 0.021 | 1000 | $1.3 \times 10^8$ | 6 | 0.2 |
| 15 | 15 | 1200 | 0.13 | 0.015 | 1470 | $2.0 \times 10^7$ | 6 | 0.17 |
| 20 | 15 | 1100 | 0.14 | 0.010 | 2300 | $3.0 \times 10^6$ | 2 | 0.15 |
| 25 | 25 | 950 | 0.13 | 0.007 | 3100 | $7.0 \times 10^5$ | 4 | 0.15 |
| 30 | 32 | 840 | 0.13 | 0.005 | 4300 | $7.8 \times 10^4$ | 2 | 0.13 |
| 35 | 45 | 750 | 0.11 | 0.003 | 6800 | $1.1 \times 10^4$ | 5 | 0.11 |

[a] Values reported are computer simulation values which gave the best fit to the real data where the association rate constants $k_{+2}$, $k_{+3}$, and $k_{+e}$ were assumed constant and equal to 1 $\mu M^{-1}$ $s^{-1}$.

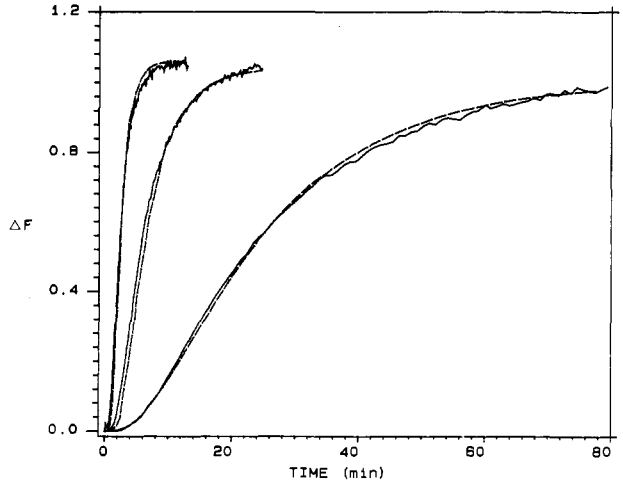


FIGURE 1: Effect of temperature on actin polymerization. The solid lines show the fluorescence increase associated with the polymerization of 23.5 $\mu$M Ca–G-actin (0.8% pyrene-labeled actin) in G buffer initiated by the addition of 2 mM $MgCl_2$. From left to right, polymerization at 30, 20, and 10 °C. The time courses at each temperature have been normalized to the same final fluorescence value. The dashed lines are computer-simulated time courses using Scheme I and the rate constants shown in Table II.

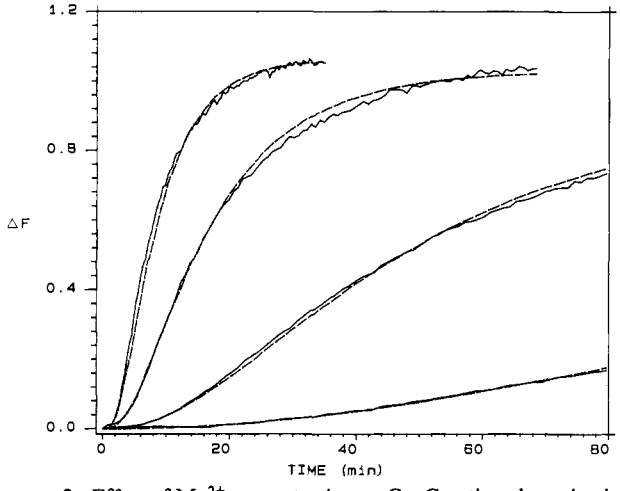


FIGURE 2: Effect of $Mg^{2+}$ concentration on Ca–G-actin polymerization at 10 °C. The solid lines show the fluorescence increase associated with the $Mg^{2+}$-induced polymerization of 23.5 $\mu$M Ca–G-actin (0.8% pyrene-labeled actin) in G buffer. From left to right, the concentrations of $MgCl_2$ added were 4, 2.5, 1.5, and 1 mM. The dashed lines are computer-simulated time courses calculated by using Scheme I and the rate constants shown in Table II.

of the lag time. Polymerization time courses in Figure 1 have been normalized to the same final fluorescence extent since the fluorescence of the pyrene probe decreased in direct proportion to temperature increase. The percent of fluorescence decrease of pyrene-labeled G-actin, however, is identical with that found for pyrene-labeled F-actin with temperature increase, suggesting the extent of fluorescence enhancement of G-actin to F-actin is identical regardless of temperature.

Representative examples of polymerization time courses at 10 °C as a function of $Mg^{2+}$, Ca–G-actin, and Mg–G-actin concentrations are shown in Figures 2, 3, and 4, respectively. The dashed curves represent the predicted time courses using Scheme I. Fits of simulated to real data similar to those shown for polymerization at 10 °C were also obtained for actin polymerizations at each of the temperatures examined. The best fits between simulated and real data gave the rate and dissociation constants summarized in Table II. For these fits, the rate constants for dimer ($k_{+2}$) and trimer ($k_{+3}$) formation, as well as filament elongation ($k_{+e}$), were assumed equal to

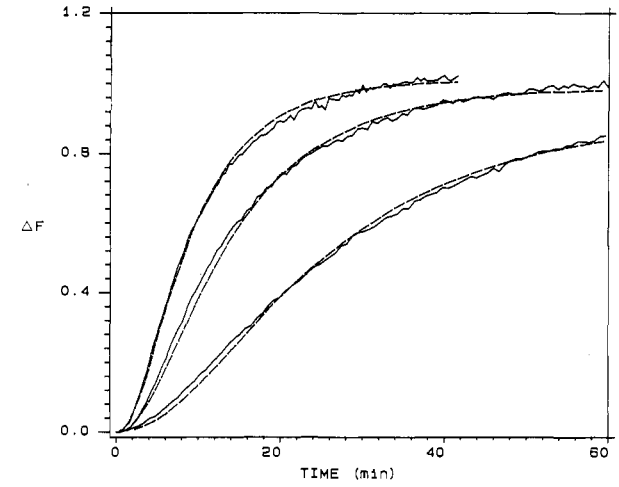


FIGURE 3: Actin polymerization at 10 °C as a function of Mg–G-actin concentration. The solid lines show the fluorescence increase associated with polymerization of Mg–G-actin monomer in 200 $\mu$M ATP, 300 $\mu$M $MgCl_2$, and 2 mM Tris buffer, pH 8, initiated by the addition of 1.7 mM $MgCl_2$ at time zero. From left to right, the actin concentrations were 30, 23.5, and 15 $\mu$M. The dashed lines are computer-simulated time courses calculated by using Scheme I and the rate constants shown in Table II.

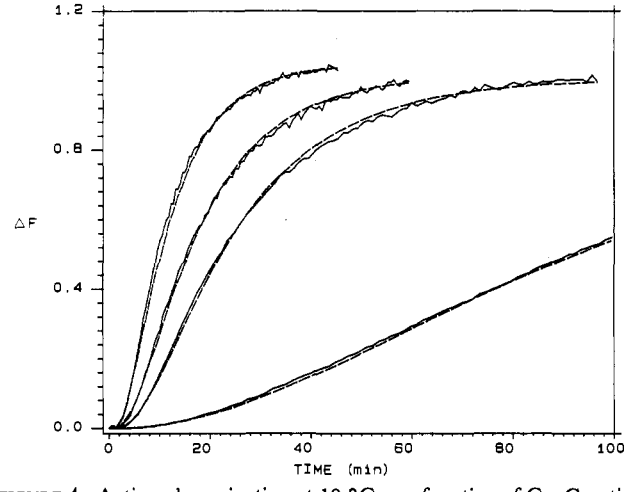


FIGURE 4: Actin polymerization at 10 °C as a function of Ca–G-actin concentration. Ca–G-actin monomer, in G buffer, was polymerized by the addition of 2 mM $MgCl_2$ at time zero (solid lines). From left to right, the actin concentrations were 40, 30, 23.5, and 10 $\mu$M. The dashed lines are computer-simulated time courses calculated by using Scheme I and the rate constants shown in Table II.

Table III: Thermodynamic Parameters

| constant | $\Delta H$ (kcal/mol) | $\Delta S$ (cal $mol^{-1}$ $K^{-1}$) | $\Delta G^a$ (kcal/mol) |
|---|---|---|---|
| $K_{Ca}$ | −14.7 | −53.7 | 1.0 |
| $K_{Mg^*}$ | 4.3 | −0.8 | 4.5 |
| $k_{+1}/k_{-1}$ | 11.7 | 45.0 | −1.5 |
| $K_{Mg2}$ | −13.0 | 59.7 | −30.5 |
| $k_{+2}/k_{-2}$ | 64.3 | 189.5 | 8.8 |
| $k_{+2}/k_{-2}^b$ | 48.8 | 134.9 | 9.3 |
| $k_{+e}/k_{-e}$ | 3.8 | 16.6 | −1.1 |

[a] Values calculated at 20 °C. [b] Corrected by assuming $k_{+e}$ changes with temperature in the same manner as found for elongation from the actin filament pointed end.

1 $\mu M^{-1}$ $s^{-1}$. This rate constant was anticipated to be near the diffusion-limited reaction rate for these reactions.

The kinetic constant determination at different temperatures allows computation of the enthalpy, entropy, and free energy changes associated with each step of the polymerization process. These thermodynamic values were obtained from slopes and intercepts of Arrhenius plots using the van't Hoff rela-

tionship. The results of these calculations have been tabulated in Table III.

## Discussion

It has been shown elsewhere (Frieden & Goddette, 1983; Frieden, 1983) that it is possible to determine the kinetic constants for individual steps (i.e., nucleation, dimerization, trimerization, and elongation) from computer simulations using the full time course of the polymerization reaction at several actin concentrations. The kinetic constants obtained by fits of $Mg^{2+}$-induced G-actin polymerizations to computer-simulated time courses indicate not only that dimer formation from monomer is highly unfavorable as previously reported for polymerization at 20 °C (Frieden, 1983) but also that it is exceedingly temperature sensitive. This equilibrium decreases 4 orders of magnitude between 10 and 35 °C. Such a large equilibrium change is highly unusual over only a 25 °C change and is considerably larger than expected for simple temperature dependence on monomer–monomer encounter rates.

Since all other equilibria change at most 7-fold over the temperature range examined (Tables I and II), the change in dimer formation is primarily responsible for the large changes in polymerization rate as a function of temperature. Indeed, the increase in polymerization rate with temperature would even be larger if not for the binding of a second mole of $Mg^{2+}$ becoming more unfavorable with increasing temperature. This increase in $K_{Mg2}$ effectively reduces the concentration of monomeric species able to form dimers under our polymerization conditions.

Stopped-flow studies of AEDANS-labeled actin (Table I) show that $K_{Ca}$ increases with increasing temperature, while the values for $K_{Mg^*}$, the binding constant for initial $Mg^{2+}$ association, and $K_{Mg1}$, the overall $Mg^{2+}$ binding constant, decrease. Furthermore, above 35 °C it appears that overall binding of $Mg^{2+}$ will be tighter than $Ca^{2+}$, while the opposite occurs as the temperature falls below 30 °C. As these ions compete for the same site on the actin molecule (Frieden, 1983), this suggests the ion binding site may become more "closed" (i.e., less internal volume) with temperature, since the atomic radius of $Mg^{2+}$ is only about two-thirds that of $Ca^{2+}$.

The constants $k_{+1}$ and $k_{-1}$, rates which describe the $Mg^{2+}$-induced actin isomerization, both decrease with increasing temperature. This implies that these constants are not true microscopic rates, which always increase with increasing temperature, but instead represent composites of at least two, and probably more, individual microscopic rates. This is not unexpected since several steps might be involved in conformational changes as a result of protein–protein and protein–water contacts being formed and broken. The equilibrium ($k_{-1}/k_{+1}$) between the two isomers of Mg–G-actin shifts toward the species represented by A′Mg (Scheme I) as the temperature rises. Since enhancement of AEDANS-labeled actin fluorescence with $Mg^{2+}$ addition is a result of A′Mg species formation, a fluorescence enhancement increase is predicted with increasing temperature. Computer simulations predict, using the rate constants found in Table I, a 1.20-fold increase in AEDANS-labeled fluorescence between 10 and 30 °C, which compares quite favorably to the observed 1.21-fold increase in fluorescence enhancement over the identical temperature range.

The equilibrium between filament elongation and disassembly ($k_{-e}/k_{+e}$) shows only a slight shift toward elongation with increasing temperature. The $k_{-e}/k_{+e}$ ratio, however, is actually a composite of at least 16 different rate constants: those for the monomer–filament equilibrium at the barbed and pointed ends of the F-actin filament and those which differ according to the state of the bound nucleotide (whether ATP or ADP) at the filament end (Frieden, 1985; Pantaloni et al., 1985). The fact that good fits to the data can be achieved by using only two rate constants suggests $k_{-e}/k_{+e}$ is an adequate description of polymer assembly and disassembly rates over the experimental conditions examined. Indeed, since the pointed end elongates at a considerably slower rate than the barbed end (Pollard & Mosseker, 1981), $k_{-e}/k_{+e}$ probably closely represents the rates at the barbed end. The value of $k_{+e}/k_{-e}$ also suggests that at steady state the bound nucleotide at the filament end is mostly ADP, since the critical concentration has been reported to be higher for a filament end containing a bound ATP (Pantaloni et al., 1985).

Elongation rate ($k_{+e}$) values between 1 and 12 $\mu M^{-1}$ $s^{-1}$ have been reported for various polymerization conditions and by various methods (Lal et al., 1984; Pollard, 1983; Bonder et al., 1983; Pollard & Mooseker, 1981). The forward rate constants for dimer formation ($k_{+2}$), trimer formation ($k_{+3}$), and filament elongation ($k_{+e}$) were assumed equal to 1 $\mu M^{-1}$ $s^{-1}$ in our initial simulations at all temperatures (Table II). This value is nearly identical with the value obtained by Lal et al. (1984) of 1.8 $\mu M^{-1}$ $s^{-1}$ whose reported conditions (1 mM $MgCl_2$, 200 $\mu M$ ATP, Tris buffer, pH 8.0 at 25 °C) are the most similar to ours.

The values reported for filament elongation are in the range usually assumed for a diffusion-controlled process. If this assumption is true, only a very small increase in $k_{+e}$ would be expected with increasing temperature. To test this, we measured actin polymerization in the presence of plasma gelsolin to obtain filament elongation rates from the pointed (slow-growing) end of the actin filament. As elongation from the pointed end is known to be slower than from the barbed end (Pollard & Mosseker, 1981), elongation from this end is the least likely to be diffusion controlled, and therefore the most likely to exhibit a larger temperature dependence. The elongation rates for this end appear to change by about 6-fold from 10 to 30 °C, with an activated enthalpy change of 14.8 kcal/mol. This value is somewhat larger than the one reported by Gershman et al. (1985) of 11 kcal/mol using phalloidin-stabilized actin nuclei and 1 mM $MgCl_2$. However, it appears this elongation rate is sensitive to $Mg^{2+}$ concentration (Doi & Frieden, 1984). The temperature dependence is also greater than that expected for a strict diffusion-controlled process (about 5 kcal/mol). Nevertheless, the change in elongation rate as a function of temperature is not large.

Since the elongation rate from the pointed end increases with increasing temperature, the assumption that $k_{+e}$ is constant over the temperature range examined is probably not true. If this is the case, it is important to know how changes involving elongation rates affect the kinetic parameters reported here. First, the value for $k_{-e}$ must change by the identical factor as $k_{+e}$ in order to achieve the same monomer–polymer equilibrium ($C_c$). Second, if $k_{+e}$ is underestimated, an identical fit to the data can be made by assuming the value for $k_{+2}$ is overestimated by the same factor. This relationship is shown graphically in Figure 5. Thus, the consequence of underestimation of the elongation rate is that dimer formation is more unfavorable than reported in Table II, depending both on the actual elongation rate value and on how it changes with temperature. The fits of the computer simulations to the real data will remain unchanged, however, as well as the temperature dependence of all other rate constants. Corrections in $k_{+e}$, $k_{-e}$, and the $k_{-2}/k_{+2}$ ratio, assuming a temperature dependence identical with that found for the pointed filament end, result

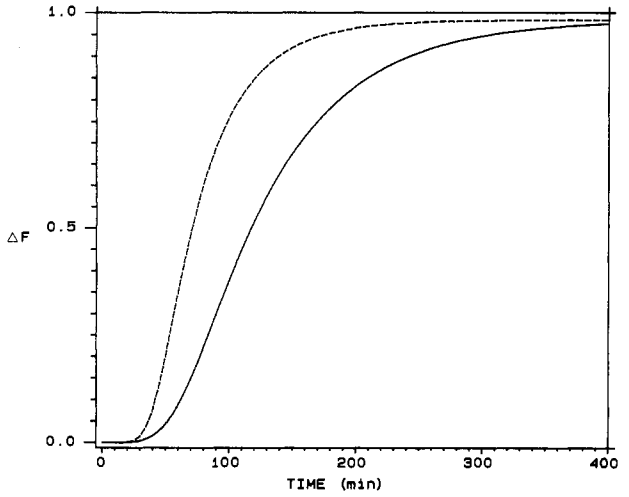


FIGURE 5: Reciprocal relationship between dimer formation and filament elongation. The right curve (solid line) is a computer-simulated polymerization in G buffer at 30 °C calculated by using Scheme I, the parameter values listed in Table II, and concentrations of 2 mM for $MgCl_2$ and 23.5 μM for Ca–G-actin. The left curve (dashed line) is the computer simulation when the rates $k_{+e}$ and $k_{-e}$ are increased 10-fold over the values used to simulate the right curve. When both the ratio between forward and reverse rate constants for dimer formation and the rates $k_{+e}$ and $k_{-e}$ are increased 10-fold, computer simulation of the full polymerization time course returns to the right curve.

Table IV: Kinetic Parameters for the $Mg^{2+}$-Induced Polymerization of Actin Corrected for Temperature[a]

| temp (°C) | $k_{+e}$ ($\mu M^{-1} s^{-1}$) | $k_{-e}$ ($s^{-1}$) | $k_{-2}/k_{+2}$ (μM) | $C_c$[b] (μM) |
|---|---|---|---|---|
| 10 | 1.0 | 0.2 | $1.30 \times 10^8$ | 0.6 |
| 20 | 2.7 | 0.4 | $8.0 \times 10^6$ | 0.5 |
| 30 | 6.0 | 0.8 | $4.6 \times 10^5$ | 0.5 |

[a] All other rates involved in Scheme I for actin polymerization remain identical with the values listed in Table II. [b] Critical concentration predicted by computer simulation using Scheme I, the rate constants in Table II, and concentrations of 200 M $Ca^{2+}$, 2 mM $Mg^{2+}$, and 23.5 μM Ca–G-actin.

in the values tabulated in Table IV.

The critical concentration ($C_c$) is the amount of G-actin in equilibrium with F-actin. It is predicted by using Scheme I and the rate constants in Table II that this value is nearly independent of temperature (Table IV). The fluorescence enhancement of pyrene-labeled actin which occurs with polymerization was also found to be independent of temperature. If the extent of fluorescence enhancement is assumed equal to the F-actin concentration, the fact this enhancement does not change with temperature supports the conclusion of computer simulations which indicate $C_c$ remains nearly unchanged between 10 and 35 °C.

Wegner and Savko (1982) reported that it was necessary to have spontaneous fragmentation of actin filaments to fit the $Mg^{2+}$-induced polymerization of actin at pH 7.5. Grazi & Trometter (1985) recently reported $Ca^{2+}$–F-actin spontaneously fragments at low temperature and went on to suggest $Mg^{2+}$–F-actin probably undergoes spontaneous fragmentation also at low temperature. We also anticipated temperature might alter the amount of spontaneous fragmentation since the kinetic energy of the filaments will be lower as the temperature decreases. Thus, less filament energy might be expected to result in less filament fragmentation. On this basis, however, it is perhaps surprising Grazi and Trometter (1985) reported higher fragmentation rates at lower temperature.

Fragmentation can be included in Scheme I by adding the step:

$$\{A'(Mg)_2\}_n \underset{k_a}{\overset{k_f}{\rightleftharpoons}} \{A'(Mg)_2\}_{2n}$$

where $k_f$ is the rate of fragmentation, $k_a$ the rate of reannealing, and $A'(Mg)_2$ the actin polymer. The addition of this step did not improve the fits between simulated and real data, however, which suggests $Mg^{2+}$–F-actin undergoes little or no spontaneous fragmentation between 10 and 35 °C at pH 8. Not only were we able to achieve good fits of the data to a mechanism which did not contain this fragmentation term but also the equilibrium constants obtained by these fits at various temperatures followed an expected van't Hoff relationship. This relationship would not be expected to hold if temperature is affecting the rate of fragmentation, and thus filament number. Therefore, if fragmentation occurs, reannealing must be rapid enough as to not alter the filament concentration.

The temperature-dependent studies of actin polymerization reported here confirm previous reports which concluded elongation ($k_{+e}$) was driven by an entropy increase sufficient to yield an overall decrease in the free energy of the system during polymerization (Swezey & Somero, 1982; Kasai, 1969). The fact that changes in entropy and enthalpy are both positive suggests monomer–filament interactions may be primarily hydrophobic, since entropy-drive processes are thought to primarily involve hydrophobic interactions (Lauffer, 1975). Hydrophobic interactions usually result in a change of the surrounding water structure which is both endothermic and characterized by positive changes in entropy. Furthermore, they are the only type of noncovalent bond which have this characteristic. These thermodynamic changes are the result of water molecules being expelled and released into the bulk solvent phase. This expulsion results in the breaking of hydrogen bonds with a concomitant increase in the degree of orientational freedom allowed. That hydrophobic effects are important in actin polymerization is further supported by a recent study by Swezey and Somero (1985) which found a positive increase in volume upon G- to F-actin transformation.

The $Mg^{2+}$-induced conformational change also appears driven by entropy, which is consistent with a change in actin conformation causing the expulsion of bound water molecules. Indeed, the thermodynamic values obtained suggest $Mg^{2+}$ may induce polymerization with a better degree than $Ca^{2+}$ simply by reducing the enthalpy and entropy change needed for dimer formation ($k_2/k_{-2}$). This suggests the $Mg^{2+}$-induced isomer may represent an intermediate between the native G-actin conformation and that of F-actin. It is interesting to speculate that $Ca^{2+}$-induced polymerization may be less efficient due to the lack of such an intermediate species.

In conclusion, the large dependence of polymerization rate with temperature is largely the result of changes in the rate of dimer formation from actin monomer. Recent preliminary evidence (C. T. Zimmerle and C. Frieden, unpublished results) suggests the effect of temperature on the rate of dimer formation may be partially correlated with a temperature-induced $pK_a$ shift in aspartic or glutamic acid residues. Preliminary fitting of actin polymerization at pH 7.0 suggests dimer formation becomes approximately 3 orders of magnitude more favorable as the pH is lowered from 8 to 7. This suggests, in turn, that the pH and temperature dependence of dimer formation may be related, with an increase in temperature resulting in an apparent increase in the $pK_a$ for some ionizable residue(s). An increase in the $pK_a$ with temperature rise suggests a negative heat of ionization. On this basis, only aspartic and glutamic acid residues, as well as the carboxy terminus, have been reported to have negative heats of ionization (Izatt & Christensen, 1975). Thus, the protonation

state of aspartic and glutamic acids may be critical for dimer formation. The fact that 23% of the primary actin sequence is composed of these residues (Elzinga et al., 1973) suggests actin would be particularly responsive to these amino acid $pK_a$'s.

## Added in Proof

Recent experiments (Carlier et al., 1986; Gershman et al., 1986; Konno & Morales, 1985) have indicated that actin contains a very tightly bound $Ca^{2+}$ ($K_d < 0.01$ $\mu$M). However, we do not believe that release of $Ca^{2+}$ from this site is related to the kinetic mechanism proposed in Scheme I. The presence of a site which binds $Ca^{2+}$ this tightly therefore does not alter the conclusions reached in this paper.

**Registry No.** Mg, 7439-95-4; Ca, 7440-70-2.

## References


Barden, J. A., & Remedios, C. G. (1985) *Eur. J. Biochem. 146*, 5–8.

Barshop, B. A., Wrenn, R. F., & Frieden, C. (1983) *Anal. Biochem. 130*, 134–145.

Bonder, E. M., Fishkind, D. J., & Mooseker, M. S. (1983) *Cell (Cambridge, Mass.) 34*, 491–502.

Bradford, M. M. (1976) *Anal. Biochem. 72*, 248–254.

Carlier, M., Pantaloni, D., & Korn, E. D. (1986) *J. Biol. Chem. 261*, 10778–10784.

Cooper, J. A., Buhle, E. L., Walker, S. B., Tsong, T. Y., & Pollard, T. D. (1983) *Biochemistry 22*, 2193–2202.

Doi, [illegible], & Frieden, C. (1984) *J. Biol. Chem. 259*, 11873–11875.

Elzinga, M., Collins, J. H., Kuehl, W. M., & Adelstein, R. S. (1973) *Proc. Natl. Acad. Sci. U.S.A. 70*, 2687–2691.

Frieden, C. (1982) *J. Biol. Chem. 257*, 2882–2886.

Frieden, C. (1983) *Proc. Natl. Acad. Sci. U.S.A. 80*, 6513–6517.

Frieden, C. (1985) *Annu. Rev. Biophys. Chem. 14*, 189–210.

Frieden, C., & Goddette, D. W. (1983) *Biochemistry 22*, 5836–5842.

Frieden, C., Lieberman, D., & Gilbert, H. R. (1980) *J. Biol. Chem. 255*, 8991–8993.

Gershman, L. C., Selden, L. A., & Estes, J. E. (1985) *Biophys. J. 47*, 120a.

Gershman, L. C., Selden, L. A., & Estes, J. E. (1986) *Biochem. Biophys. Res. Commun. 135*, 607–614.

Grazi, E., & Trombetta, G. (1985) *Biochem. J. 232*, 297–300.

Harris, D. E., & Schwartz, J. H. (1981) *Proc. Natl. Acad. Sci. U.S.A. 75*, 6798–6802.

Harris, H. E., & Weeds, A. G. (1983) *Biochemistry 22*, 2728–2741.

Houk, T. W., Jr., & Ue, K. (1974) *Anal. Biochem. 57*, 453–459.

Izatt, R. M., & Christensen, J. J. (1975) in *Handbook of Biochemistry and Molecular Biology: Physical and Chemical Data* (Fasman, G. D., Ed.) Vol. 1, CRC Press, Cleveland, OH.

Kasai, M. (1969) *Biochim. Biophys. Acta 180*, 399–409.

Kasai, M., Asakura, S., & Oosawa, F. (1962) *Biochim. Biophys. Acta 57*, 13–21.

Konno, K., & Morales, M. (1985) *Proc. Natl. Acad. Sci. U.S.A. 82*, 7904–7908.

Kouyama, T., & Mihashi, K. (1980) *Eur. J. Biochem. 114*, 33–38.

Lal, A. A., Brenner, S. L., & Korn, E. D. (1984) *J. Biol. Chem. 259*, 1441–1446.

Lauffer, M. A. (1975) *Mol. Biol., Biochem. Biophys. 20*, 264.

Oosawa, F., & Kasai, M. (1962) *J. Mol. Biol. 4*, 10–21.

Pantaloni, D., Carlier, M., & Korn, E. D. (1985) *J. Biol. Chem. 260*, 6572–6578.

Pollard, T. D. (1983) *Anal. Biochem. 134*, 406–412.

Pollard, T. D., & Mooseker, M. (1981) *J. Cell Biol. 88*, 654–659.

Roustan, C., Benyamin, Y., Boyer, M., Bertrand, R., Audermard, E., & Jauregui-Adell, J. (1985) *FEBS Lett. 181*, 119–123.

Spudich, J. A., & Watt, S. (1971) *J. Biol. Chem. 246*, 4866–4871.

Swezey, R. R., & Somero, G. N. (1982) *Biochemistry 21*, 4496–4503.

Swezey, R. R., & Somero, G. N. (1985) *Biochemistry 24*, 852–860.

Tait, J. F., & Frieden, C. (1982) *Arch. Biochem. Biophys. 216*, 133–144.

Tawada, K., Wahl, P., & Auchet, J. C. (1978) *Eur. J. Biochem. 88*, 411–419.

Tellam, R., & Frieden, C. (1982) *Biochemistry 21*, 3207–3214.

Wegner, A., & Engel, J. (1975) *Biophys. Chem. 3*, 215.

Wegner, A., & Savko, P. (1982) *Biochemistry 21*, 1909–1913.